

# Theoretical and experimental investigation of surface generation in swing precess bonnet polishing of complex three-dimensional structured surfaces

Chi Fai Cheung<sup>\*1</sup>, Zhong-Chen Cao<sup>\*1</sup>, Lai Ting Ho<sup>1</sup> and Ming Yu Liu<sup>1</sup>

*1. Partner State Key Laboratory of Ultra-precision Machining Technology, Department of Industrial and Systems Engineering, The Hong Kong Polytechnic University, Hung Hom, Kowloon, Hong Kong*

*\*Corresponding author: Tel.: +852 2766 7905; fax: +852 2362 5267. Email: Benny.Cheung@polyu.edu.hk (C.F. Cheung),*

*charles.cao@connect.polyu.hk (Zhong-Chen Cao).*

## Abstract

Three-dimensional structured surfaces (3D-structured surfaces) possessing specially designed functional textures are widely used in the development of advanced products. This paper presents a novel swing precess bonnet polishing (SPBP) method for generating complex 3D structured surfaces which is accomplished by the combination of specific polishing tool orientation and tool path. The SPBP method is a sub-aperture finishing process in which the polishing spindle is swung around the normal direction of the target surface within the scope of swing angle while moving around the center of the bonnet. This is quite different from the ‘single precess’ and ‘continuous precessing’ polishing regime, in which the precess angle is constant. The technological merits of the SPBP were realized through a series of polishing experiments. The results show that the generation of complex 3D-structured surfaces is affected by many factors which include point spacing, track spacing, swing speed, swing angle, head speed, tool pressure, tool radius, feed rate, polishing depth, polishing cloth, polishing strategies, polishing slurry, etc. To better understand and determine the surface generation of complex 3D-structured surfaces by the SPBP method, a multi-scale material removal model and hence a surface generation model have been built for characterizing the tool influence function and predicting the 3D-structured surface generation in SPBP based on the study of contact mechanics, kinematics theory, abrasive wear mechanism, and the convolution of the tool influence function and dwell time map along the swing precess polishing tool path. The predicted results agree reasonably well with the experimental results.

**Keywords:** Swing precess bonnet polishing; Modeling and simulation; Material removal characteristics; Surface generation; Complex 3D structured surfaces; ultra-precision machining

## 1. Introduction

Three-dimensional structured surfaces (3D-structured surfaces) are surfaces possessing specially designed functional textures which are widely used in the development of products such as compound eye lenses and diffractive elements for optics applications. To reduce adhesion in the die and mould industry, structured surfaces with a width of 2.0 mm and depth of 0.2 mm were intentionally machined [1]; 500- $\mu$ m shark skin-like structures reduce wall shear stress [2]; pore surface can enhance the load capacity and stiffness of the fluid film between the seal-mating rings [3]. Currently, 3D-structured surfaces are manufactured by different methods such as electroforming [4] and laser machining [5, 6], micro-milling [7] or micro-grinding processes [8], etc. However, it is hard to control the form error and surface texture at different areas of complex 3D-structured surfaces by using these methods. This is particularly true for the generation

of complex 3D-structured surfaces for functional applications such as wettability and lubrication.

During the past decades, much research work has been undertaken on the study of surface generation in computer controlled polishing (CCP) [9, 10] and polishing mechanics [11, 12]. Currently, CCP is found to be used to reduce surface roughness [13, 14] and figuring of aspheric and freeform surfaces [15]. However, the use of CCP for the generation of complex 3D-structured surfaces for functional applications has received relatively little attention. Although some previous research has been found for generating 3D-structured surface by computer controlled ultra-precision polishing (CCUP), it mainly focused on the generation of simple 3D-structured surfaces based on single precess polishing [16]. Stout and Blunt [17] stated that there is great demand in structured engineered parts. In order to reduce the manufacturing cost and find out more potential structures, it is necessary to explore more manufacturing processes to generate different 3D-structured surfaces. There is a need for the development of a new and controllable polishing process to generate complex 3D-structured surfaces to meet the demand for functional applications.

This paper presents the development of a novel swing precess bonnet polishing (SPBP) method for generating complex 3D-structured surfaces. The technological merits of the SPBP were realized through a series of polishing experiments and characterization tests. To better understand and determine the surface generation of complex 3D-structured surfaces by the SPBP method, a multi-scale material removal model and a surface generation model were developed and experimentally verified.

## 2. Swing precess bonnet polishing (SPBP)

### 2.1. Principle of swing precess bonnet polishing

It is well-known that surface generation by bonnet polishing is dominated by the influence function of the polishing tool instead of the pure geometry of the cutting tool that is quite different from other ultra-precision machining processes such as single-point diamond turning and ultra-precision raster milling. Taking the advantages of high polishing efficiency and flexibly controlled influence function in the bonnet polishing process, a novel swing precess bonnet polishing (SPBP) process is presented for generating complex 3D-structured surfaces which is accomplished by a combination of specific polishing tool orientation and tool path. As shown in Figure 1, the SPBP method is a sub-aperture finishing process in which the polishing spindle is swung around the normal direction of the target surface within the scope of swing angle while moving around the center of the bonnet. This is quite different from the ‘single precess’ (see Figure 2 (a)) and ‘continuous precessing’ (see Figure 2 (b)) polishing regime [18], in which the precess angle is constant.

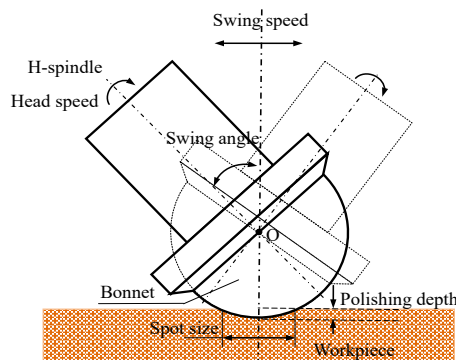


Figure 1. Schematic diagram of swing precess bonnet polishing

Figure 2 (c) and Figure 2(d) show two types of swing precess bonnet polishing processes which include climb and vertical swing precess bonnet polishing processes. In the vertical swing precess bonnet polishing process, the swing plane of polishing spindle is perpendicular to the feed direction of the polishing tool; while the swing plane of polishing spindle consists of the normal direction of the target surface and the feed direction of the polishing tool in climb swing precess bonnet polishing. The generation of complex 3D-structured surfaces is affected by many factors which include point spacing, track spacing, swing speed, swing angle, head speed, tool pressure, tool radius, feed rate, polishing depth, polishing cloth, polishing strategies, polishing slurry, etc.

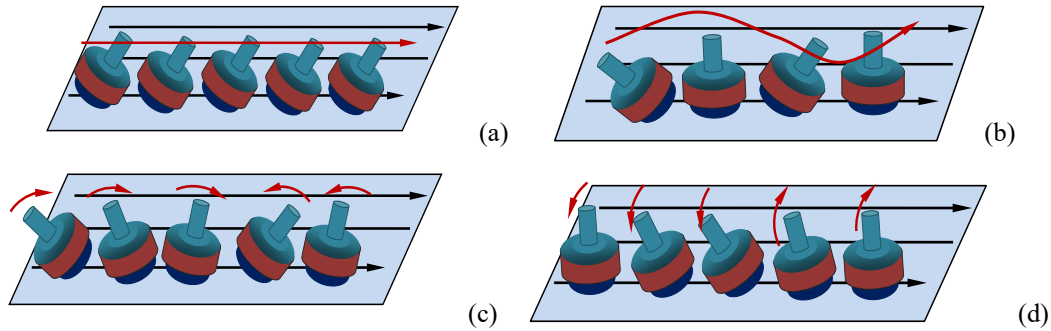


Figure 2. (a) single precess, (b) continuous precess, (c) climb and (d) vertical swing precess bonnet polishing across the raster tool path

## 2.2. Tool path generator for swing precess bonnet polishing

To realize swing precess bonnet polishing (SPBP), a tool path generator (TPG) has been purposely built which is used for generating the CNC files for polishing as shown in Figure 3. The TPG is composed of three modules which are input module, processing module, and output module. The input module is used to acquire the polishing parameters (e.g. head speed, spacing, tool pressure, bonnet radius, feed rate, etc.) and the polishing strategies (e.g. spacing and swing speed). Hence, the processing module determines the spot size, track coordinates, polishing gesture, and control parameters. The necessary CNC file of the SPBP tool path is generated by the output module. In this study, the TPG has been developed by the MATLAB programming software package. Hence, SPBP can be undertaken by a 7-axis polishing machine through two kinds of motions which include feed motion (X,Y,Z,C-axis) and swing motion (A,B,H-axis), respectively.

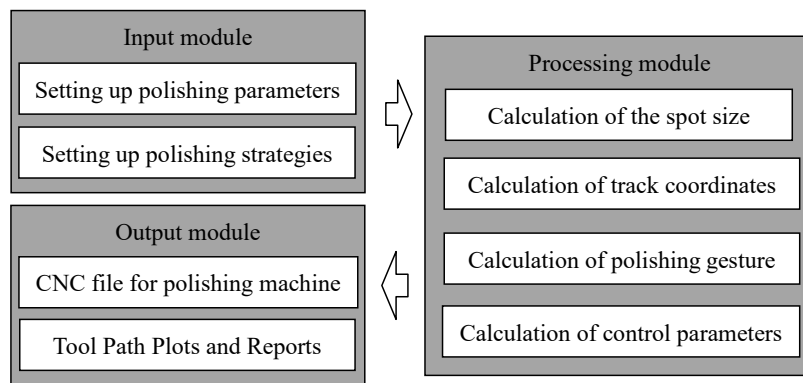


Figure 3. Schematic diagram of tool path generator for SPBP

### 3. Multi-scale modeling of material removal and surface generation of swing precess bonnet polishing

#### 3.1. Multi-scale material removal model

The surface generation of the polishing process can be regarded as the convolution of the influence function and the dwell time map along the pre-specific tool path [19]. To simulate the generation of 3D-structured surfaces by SPBP, a multi-scale material removal model has been developed based on the prior work done by the authors [20]. The model is used for predicting the tool influence function in SPBP based on the study of contact mechanics, kinematics theory, and abrasive wear mechanism. The material removal of the SPBP can be expressed by,

$$MRR(x, y, t) = \frac{2\eta K_{ac} V_c t V_r(x, y) P(x, y)}{H_w \tan \alpha} \left( \frac{R_a}{\sigma_z} \right)^{1/2} \quad (1)$$

where  $\eta$  is the volume fraction of a wear groove removed as wear debris,  $K_{ac}$  is the coefficient related to the particle size distribution and the hydrodynamics condition,  $V_c$  is the volume fraction of the polishing slurry,  $t$  is the polishing time,  $H_w$  is the hardness of polished workpiece,  $\alpha$  is the semi-angle of the cone particle,  $R_a$  is the radius of the pad asperities,  $\sigma_z$  is the standard deviation of asperity heights,  $V_r(x, y)$  is the relative velocity distribution between the polishing pad and the target surface in the polishing area, and  $P(x, y)$  is the pressure distribution at the polishing contact area.

$$V(x, y, S, \varphi, R_b, d) = \frac{\pi S}{30} \sqrt{(y \cot \varphi - (R_b - d))^2 (\sin \varphi)^2 + x^2 (\cos \varphi)^2} \quad (2)$$

where  $x^2 + y^2 \leq (R_b)^2 - (R_b - d)^2$ ;  $S$  is angular velocity in rpm;  $\varphi$  is the swing angle;  $d$  is the polishing depth in mm;  $R_b$  is the radius of the bonnet in mm.

$$P(x, y, R_b, d, \omega, Y, \nu, \varphi, \eta_1, \eta_2) = p_0 \left( 1 - \frac{x^2}{a^2} - \frac{y^2}{a^2} \right)^{1/2} + \frac{(1-2\nu)(1+\nu)}{Y} \cdot \frac{\omega \cos \varphi (2\eta_2 + \eta_1 / 3) p_0 x (R_b - d)}{a^2} \\ \cdot \left( 1 - \frac{x^2}{a^2} - \frac{y^2}{a^2} \right)^{-1/2} + \frac{(1-\nu)^2}{Y} \cdot \frac{\omega \cos \varphi (2\eta_2 + \eta_1 / 3) \pi p_0 x}{2a} \quad (3)$$

where  $a = \sqrt{dR_b}$  denotes the radius of contact area,  $Y$  and  $\nu$  are Young's modulus and the Poisson ratio, respectively, while  $\eta_1$  and  $\eta_2$  are the coefficients of viscosity related to shear and bulk deformation, respectively.  $\omega$  is the angular velocity, and  $p_0 = 3F_N / (2\pi a^2)$  denotes the maximum contact pressure,  $F_N$  is the total elastic force, acting on the surface (in normal direction) on the polishing pad:

$$F_N = \frac{2}{3} \frac{Y}{(1-\nu^2)} R_b^{1/2} d^{3/2} \quad (4)$$

#### 3.2. Surface generation model of swing precess bonnet polishing

A surface generation model has been developed for swing precess bonnet polishing based on the surface generation mechanism of the relative and cumulative removal process in the polishing process, together with the predicted tool influence function by the multi-scale material removal model as described in section 3.1. As shown in Figure 4, the track coordinates of the polishing bonnet, along with the polishing path, are determined in terms of polishing parameters and strategies. The tool influence function of every polishing point is then computed by the multi-scale material removal model with respect to the corresponding polishing gesture and track coordinates. Hence, the surface generation

by SPBP is simulated by the aggregation of the amount of material removal of the superposed tool influence function at every sampling point, together with a Gaussian Process model [21].

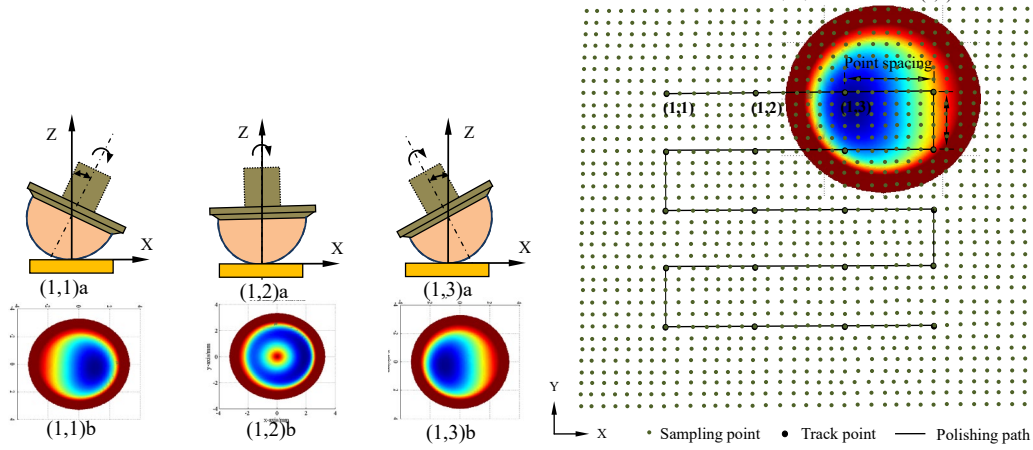


Figure 4. Schematic diagram of the surface generation mechanisms of swing precess bonnet polishing across the raster tool path

#### 4. Experimental and simulated results

To realize the technological merits as well as the performance of the multi-scale material removal model and the surface generation model for swing precess bonnet polishing, three groups of experiments (i.e. Group A, Group B and Group C) were conducted on a Zeeko IRP 200 ultra-precision freeform polishing machine, as shown in Figure 5(a). Cylindrical Nickel copper samples with a diameter of 25.4 mm were machined by single-point diamond turning to ensure their consistent initial surface finish. The parameters used in single-point diamond turning include spindle speed: 1500rpm, feed rate: 8 mm per min, depth of cut: 4  $\mu\text{m}$  and tool radius: 2.47315 mm. The surface roughness and 3D-surface topography of the samples were measured by a Zygo Nexview 3D Optical Surface Profiler. As shown in Figure 5(b), the arithmetic roughness,  $R_a$ , of the samples before polishing is found to be 103 nm.

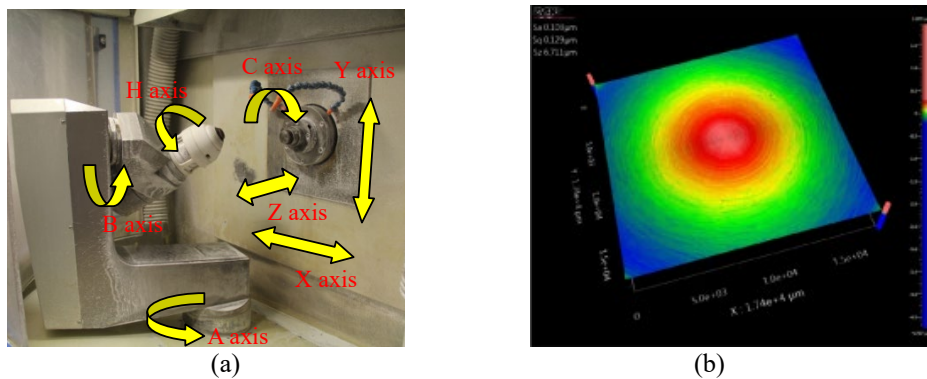


Figure 5. (a) Zeeko IRP200 Ultra-precision freeform polishing machine and (b) measured surface topography of the samples before polishing

In Group A of experiments, line tests of swing precess bonnet polishing were conducted with different polishing parameters in order to study the effect of polishing parameters on the generation of structured surfaces. Experiments conducted in Part B are pattern tests which aim to verify the feasibility of the proposed SPBP method under various polishing conditions. In Group C, experiments were undertaken to evaluate the performance of the multi-scale material removal model and surface generation model for the SPBP.

## 4.1 Group A: Effect of parameters on the generation of structured surfaces

### 4.1.1 Experimental setup

This group of experiments aims to investigate how single process parameter affects the generation of 3D-structured surface with swing precess bonnet polishing. The tool pressure and the spindle speed are 1.2 bar and 1500 rpm respectively. Other polishing settings are shown in Table 1. As shown in Figure 6, the 3D-structure surfaces generated on the polished area were characterized by peak-to-valley height (PV), the width and the length of a rectangle that can cover a cycle of the structure.

Table 1 Polishing parameters used in line tests of swing precess bonnet polishing

Sample No.	Parameters					
	Precess angle (°)	Tool offset (mm)	Feed rate (mm per min)	Spacing (mm)	Swing speed (degrees per minute)	Swing direction
1	5	0.28	50	0.4	250	Climb
2	10					
3	12					
4	10	0.14				
5		0.42				
6		0.28	25			
7			75			
8			50	0.6		
9				0.8		
10				0.4	200	
11					300	
12					250	Vertical

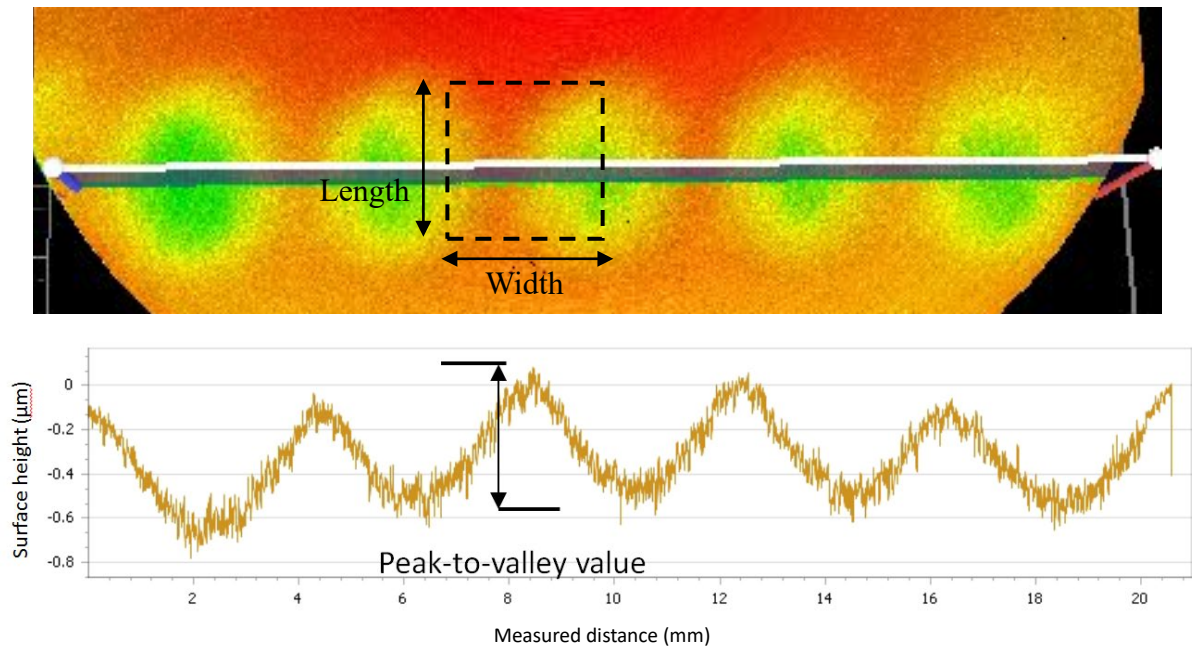


Figure 6. Characterization of the surface feature parameters of the generated 3D-structured structures



4.1.2 Results and discussion

Table 2 to Table 7 show the 3D-structures generated by only a single one-way tool path. It is interesting to note that the shape of each cycle of the structures. It is believed that this may affect the pattern of the 3D-structures formed on a surface. Precess angles and feed rate affect the density of the 3D-structures. The smaller the precess angle and the slower the feed rate, the higher the density of the 3D-structures.

Table 2 Structures generated by precess angle 5°, 10° and 15°

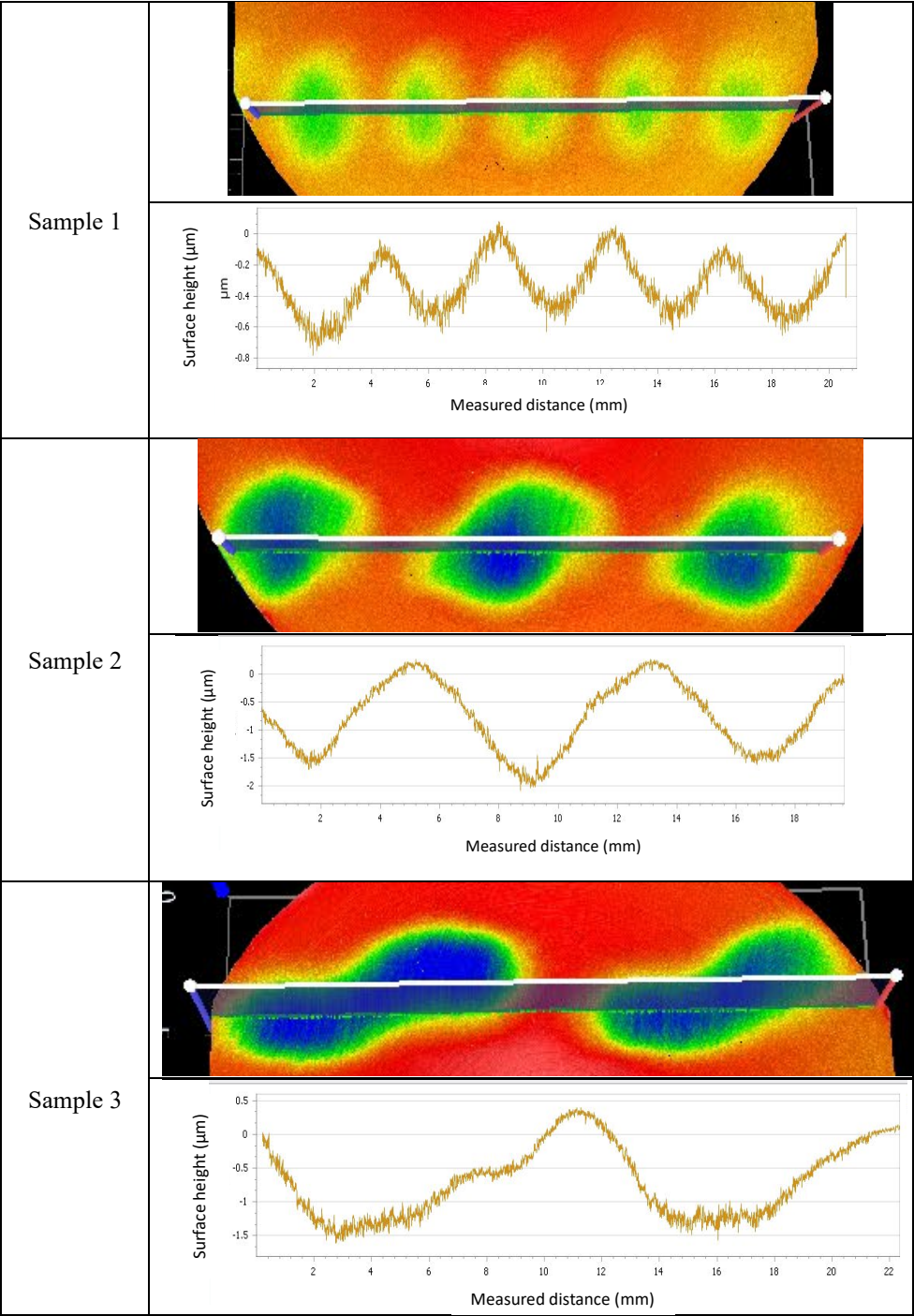


Figure 7 to Figure 12 present the peak-to-valley height (PV) values, width and length of a cycle of the 3D-structures. The PV values of precess angle 5° and feed rate 25 mm per min are relatively low. Precess angle 15°, feed rate 75 mm per min and swing speed 200 degrees per minute give similar 3D-structures, which have a larger width to length ratio. Precess angle 15° and feed rate 75 mm/min give large PV values. The PV values of tool offset of 0.14 mm is obviously smaller than that of 0.28 mm and 0.42 mm, while they give similar PV values. The swing directions only affect the shape of the 3D-structure but no obvious influence on the PV values.

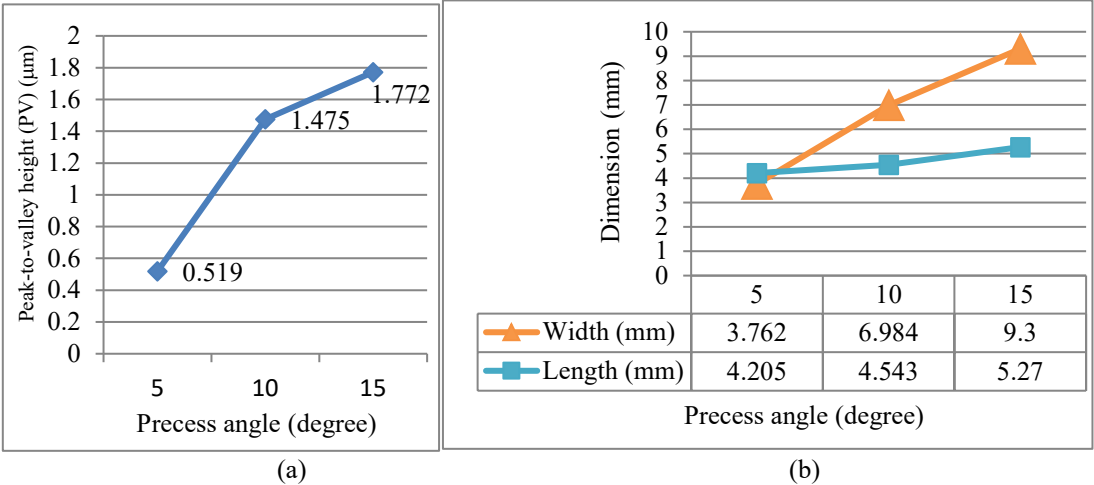
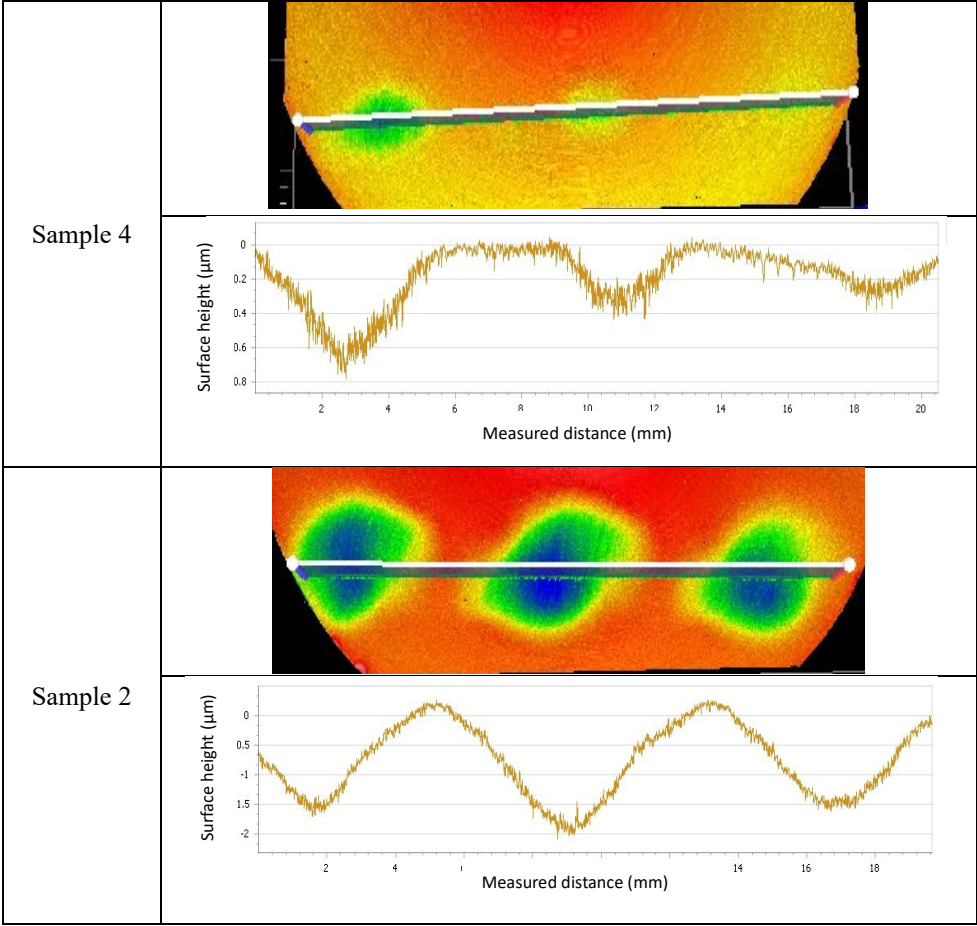


Figure 7 Effect of precess angle on the surface generation in line test: (a) peak-to-valley height (PV) and (b) width and length of the 3D-structures

Table 3 Structures generated by tool offset 0.12 mm, 0.28 mm and 0.42 mm





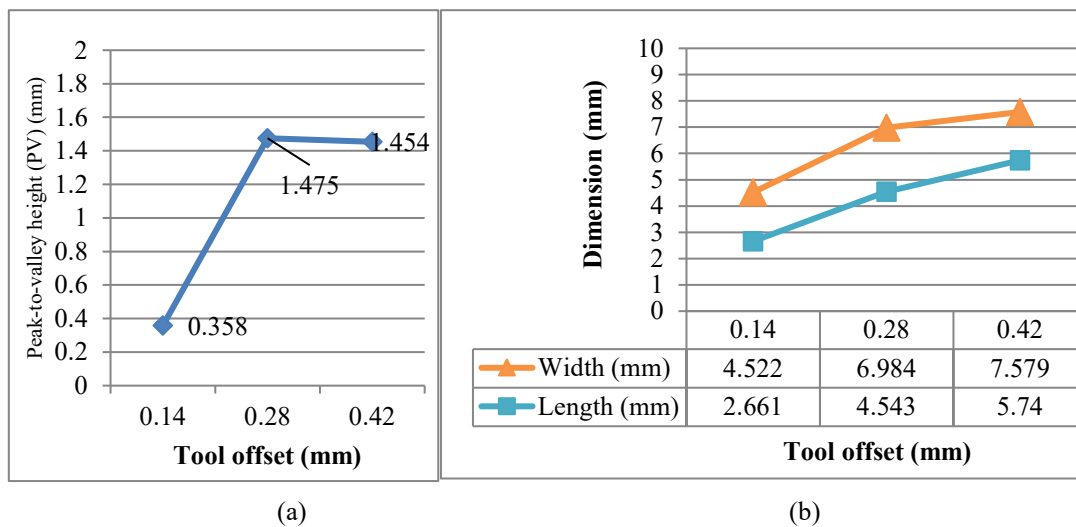
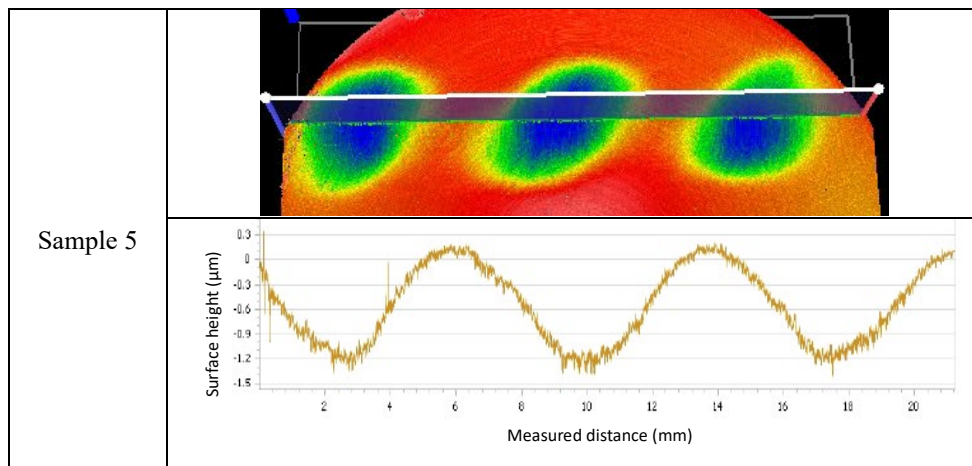
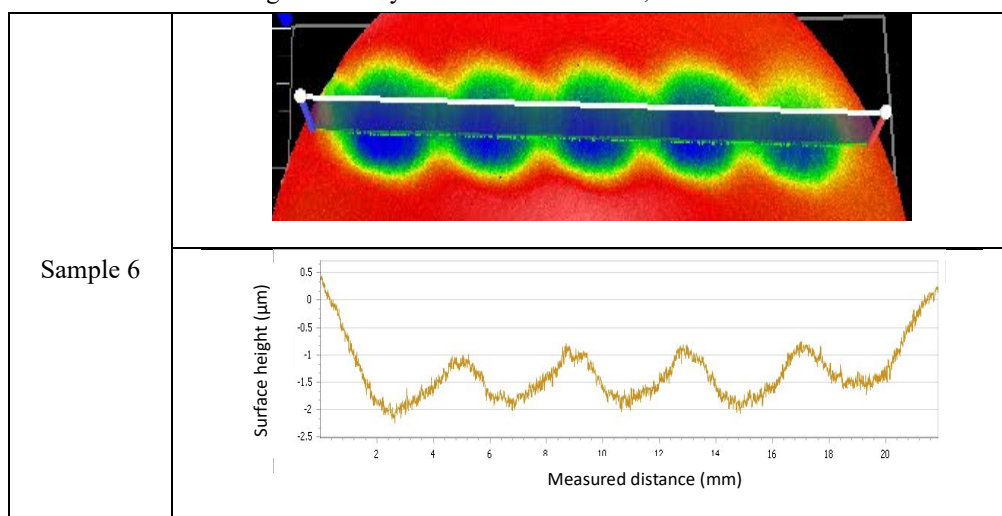


Figure 8 Effect of tool offset on the surface generation in line test: (a) peak-to-valley height (PV) and (b) width and length of the 3D-structures

Table 4 Structures generated by feed rates 25 mm/min, 50 mm/min and 75 mm/min



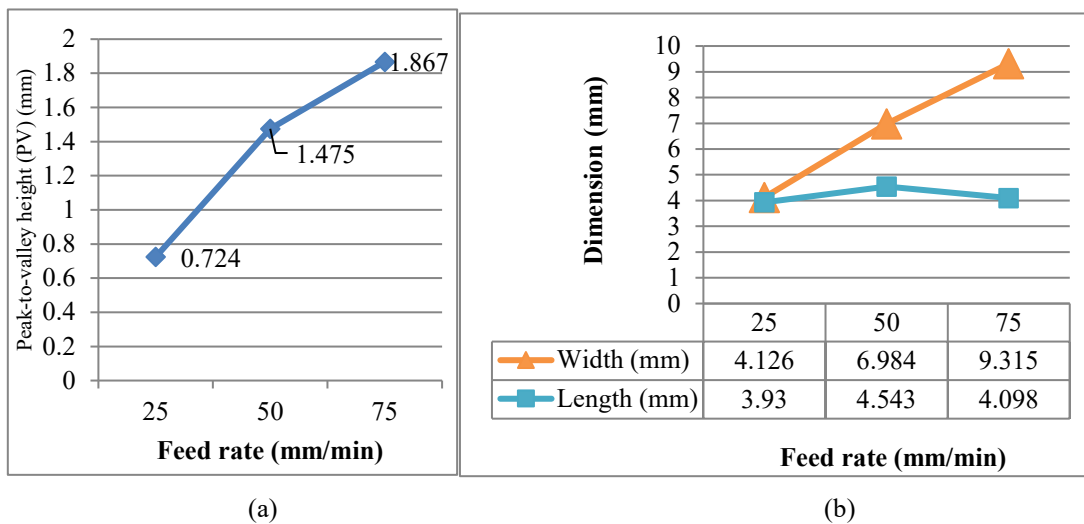
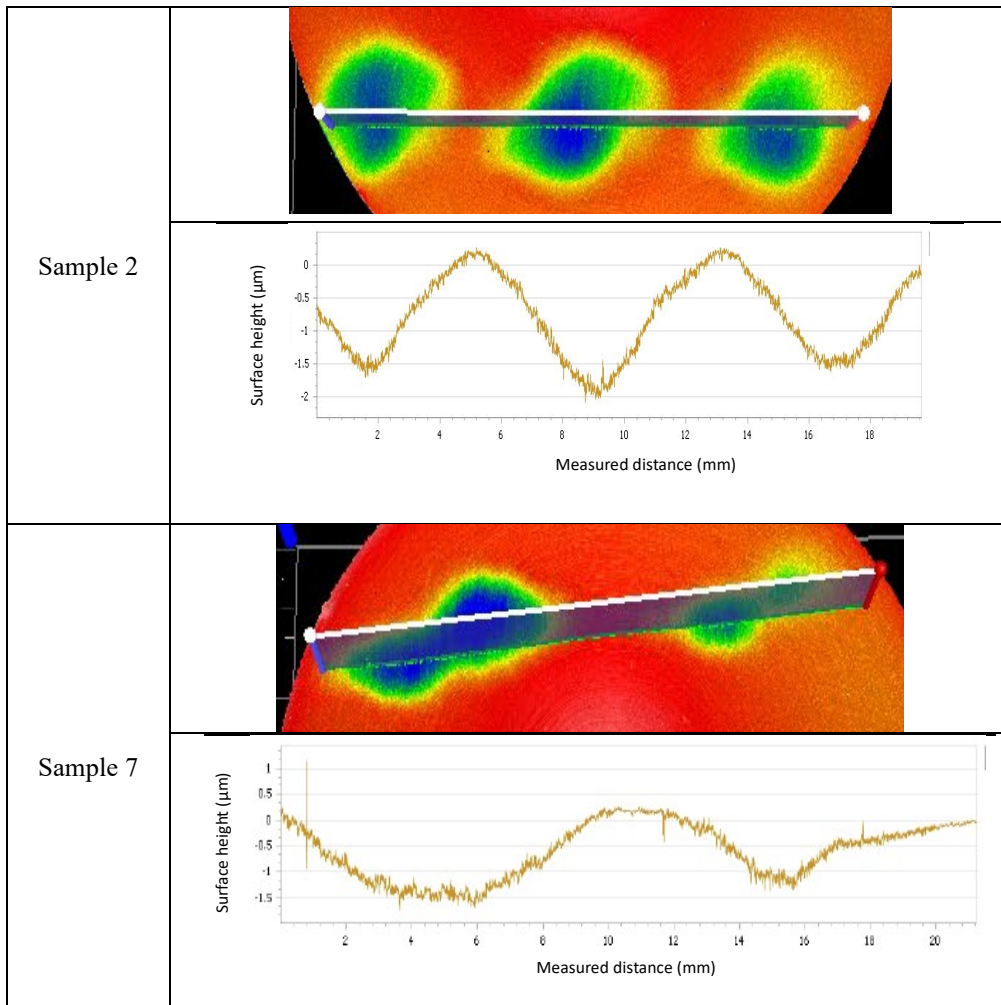
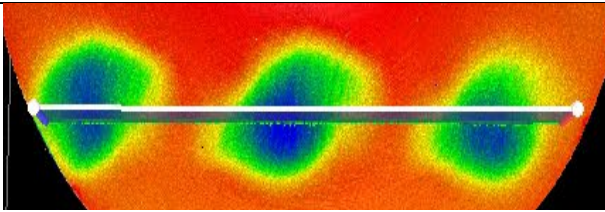
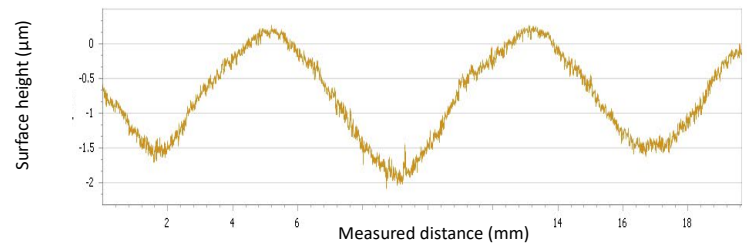
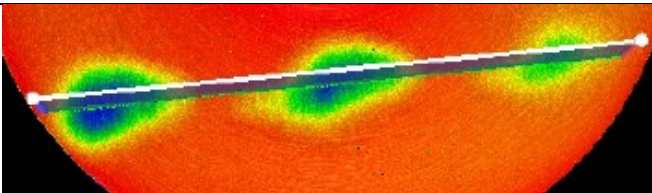
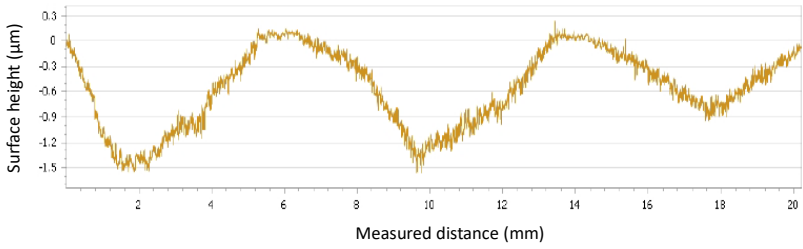
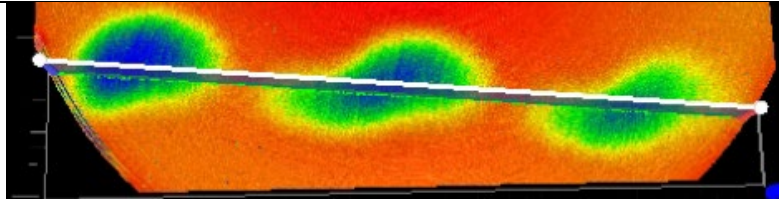
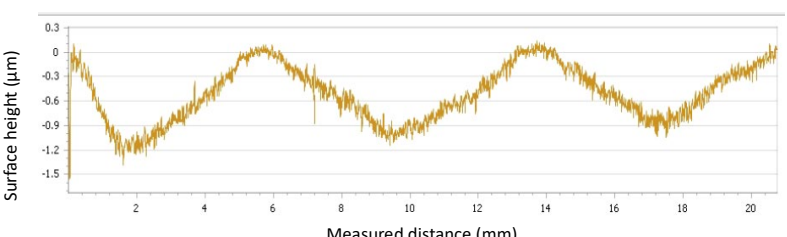


Figure 9 Effects of feed rate on the surface generation in line test: (a) peak-to-valley height (PV) and (b) width and length of the 3D-structures

Table 5 Structures generated by point spacing 0.4 mm, 0.6 mm and 0.8 mm

Sample 2	 
Sample 8	 
Sample 9	 

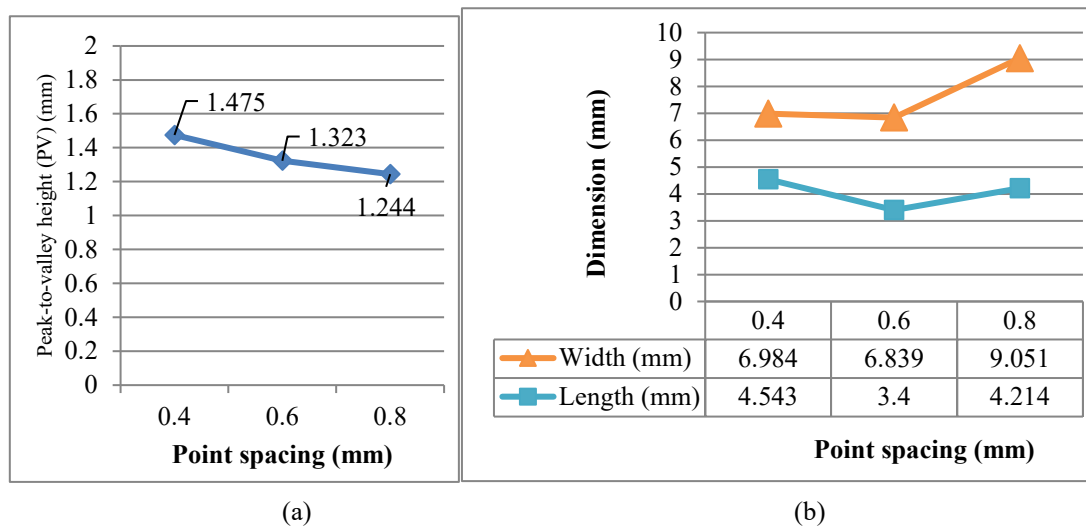
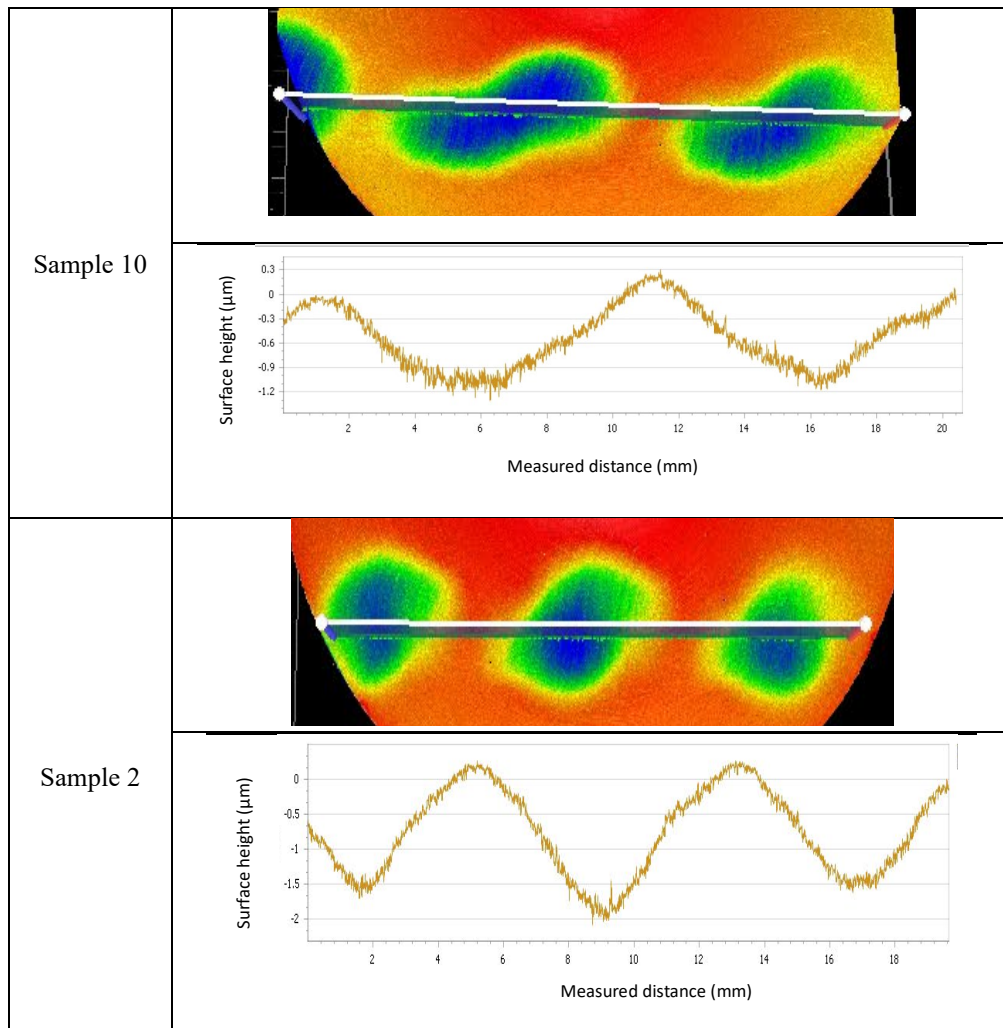


Figure 10 Effects of point spacing on the surface generation in line test: (a) peak-to-valley height (PV) and (b) width and length of the 3D-structures

Table 6 Structures generated by swing speed 200, 250 and 300 degrees per minute



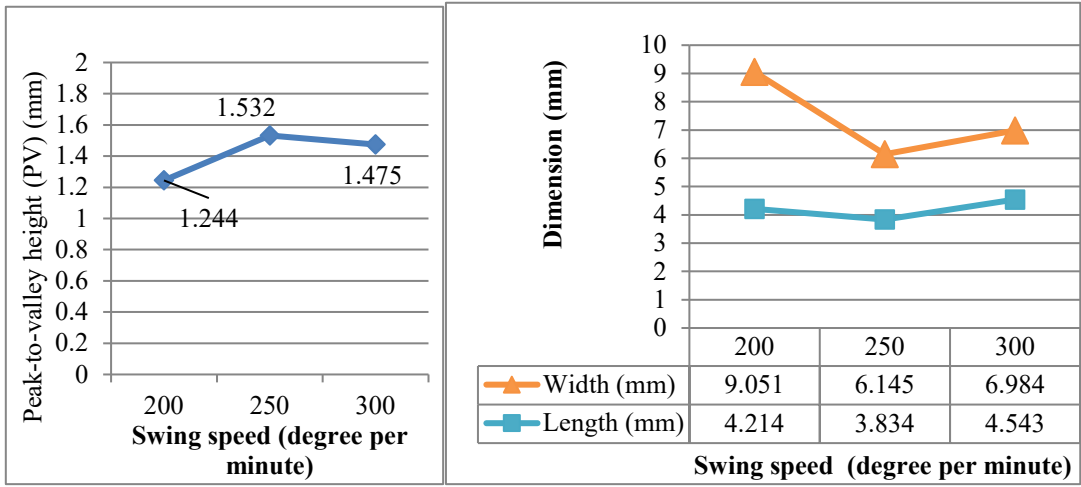
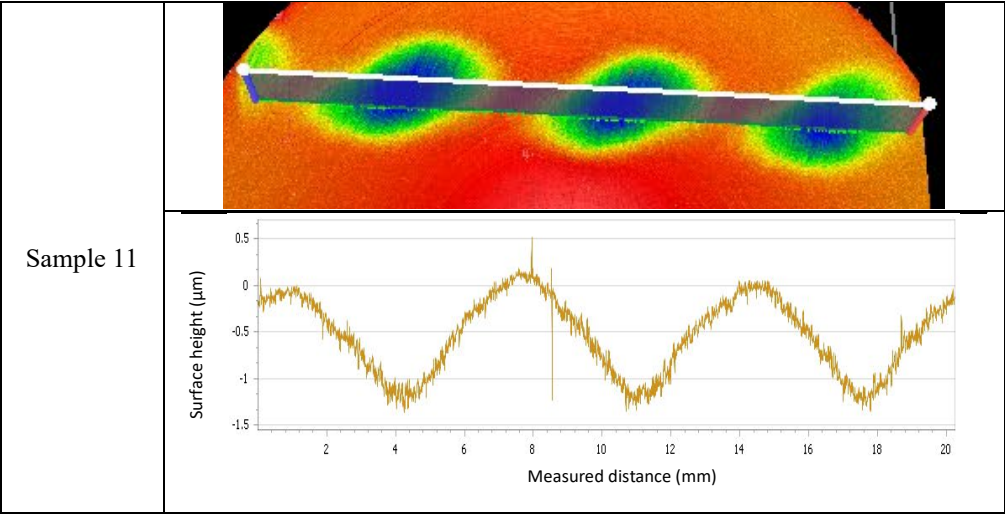
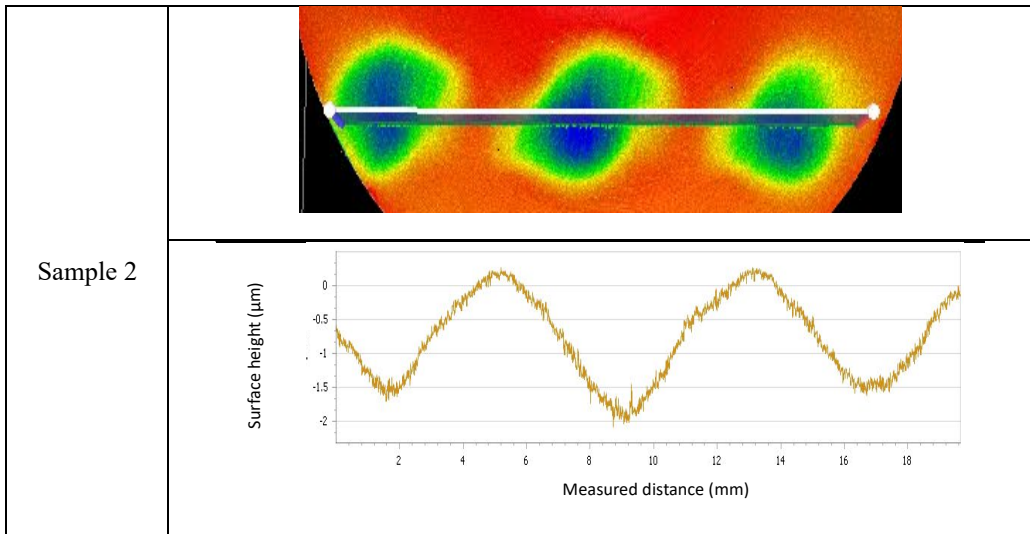


Figure 11 Effects of swing speed on the surface generation in line test: (a) peak-to-valley height (PV) and (b) width and length of the 3D-structures

Table 7 Structures generated by different swing directions





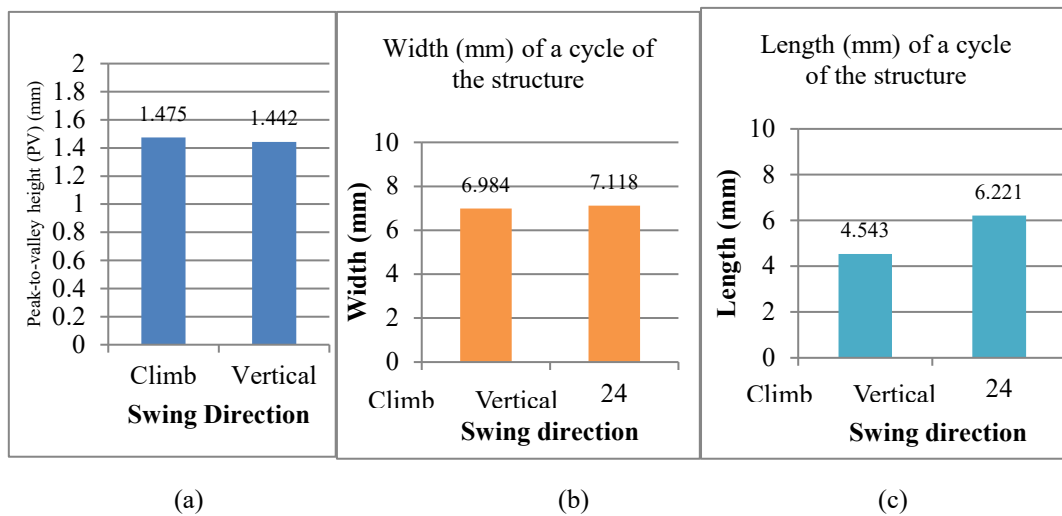
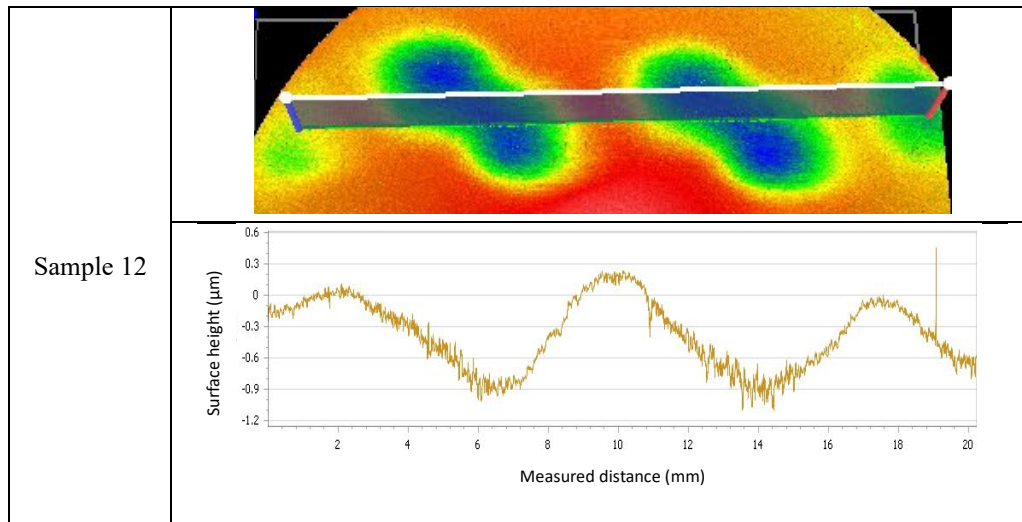


Figure 12 Effects of swing direction on the surface generation in line test: (a) peak-to-valley height (PV) , (b) width and (c) length of the 3D-structures

#### 4.2 Group B: Results of experimental investigation of pattern tests

In Group B, four sets of parameters were selected to generate 3D-structured surfaces, as shown in Table 8. The tool pressure and the spindle speed were set at 1.2 bar and 1500 rpm, respectively. Twelve samples were polished with 3 samples for each set.

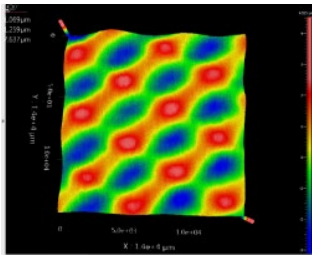
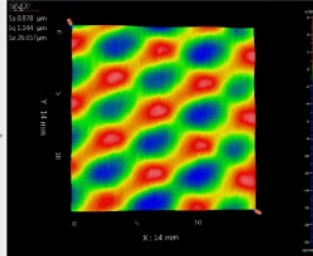
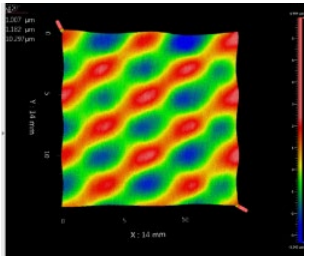
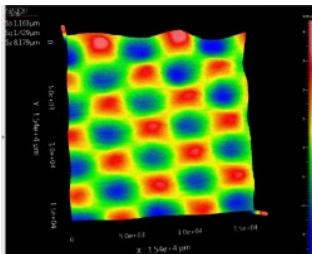
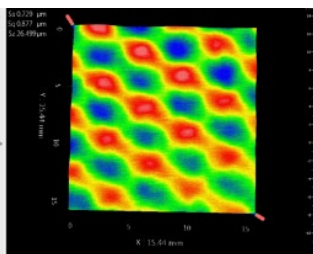
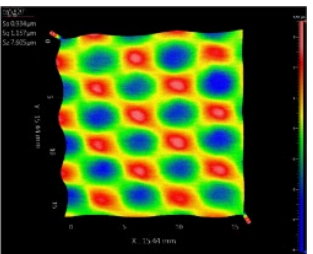
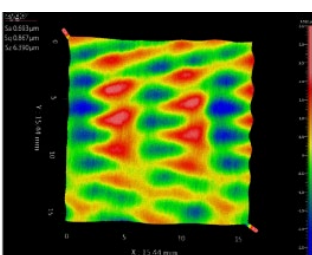
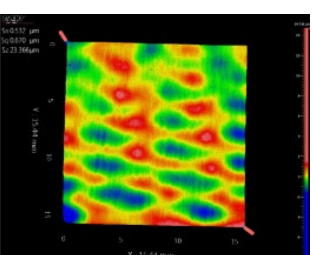
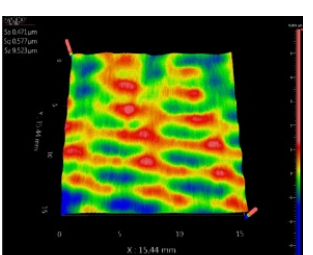
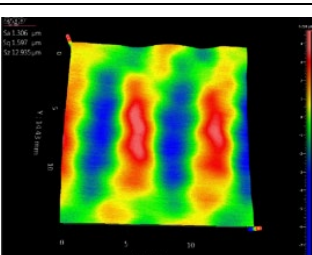
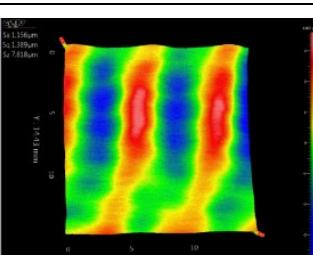
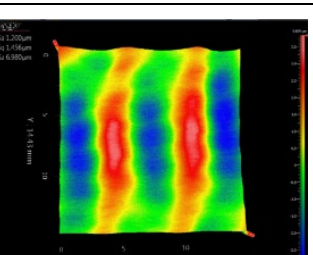
Table 8 Polishing parameters used in pattern tests of swing precess bonnet polishing

Parameter set no.	Parameters					
	Precess angle (°)	Tool offset (mm)	Feed rate (mm/min)	Spacing (mm)	Swing speed	Swing direction
1	10	0.28	50	0.4	300	Climb
2						24
3	15			0.6	250	13
4						24



Table 9 shows the results of pattern tests measured by a Zygo Nexview 3D Optical Surface Profiler and Table 10 shows the photos of the patterns generated by swing precess bonnet polishing. It is interesting to note that complex 3D-structured patterns are formed on the surfaces. The results show that different kinds of the complex 3D-structured surfaces can be generated by using different polishing parameters. It is also found that, the 3D-topographies of the 3D-structured patterns generated on the surfaces have a good consistency in surface shape when using the same polishing parameters.

Table 9 Measured topography of structured pattern generated by swing precess bonnet polishing

set no.	3D surface topography measured by a Zygo Nexview 3D Optical Surface Profiler		
	a	b	c
1			
2			
3			
4			

To further evaluate the feasibility and stability of the proposed SPBP method, the deviation of measured results with same polishing conditions was evaluated by the repeatability test. For every set of experiment, three measurement data were obtained, named set a, set b and set c. The measurement data set a was used as the reference data. Then measurement data set b and measurement data set c were compared to the reference data. The error maps were then

obtained and the root-mean-square (RMS) value of the error maps were calculated and shown in Table 11. As shown in Table 12, the result shows that the RMS values of the error maps vary from 0.2  $\mu\text{m}$  to 0.5  $\mu\text{m}$  which demonstrate that the repeatability of the experiment is quite well. This implies that swing precess bonnet polishing can be used for generating different kinds of 3D-structured patterns in deterministic and stable way.

Table 10 Photos of structured pattern generated by swing precess bonnet polishing

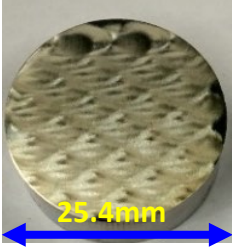
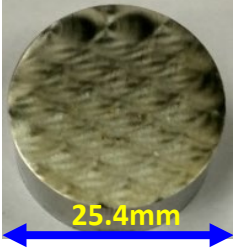
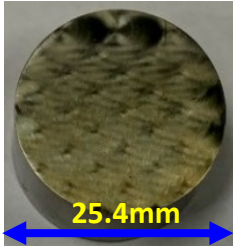
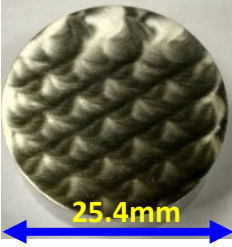
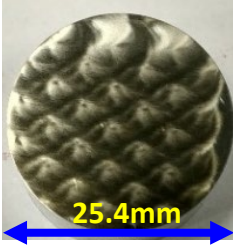
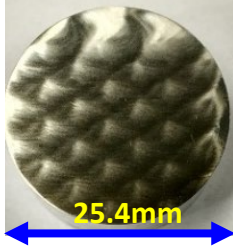
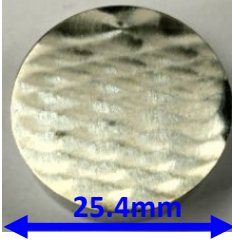
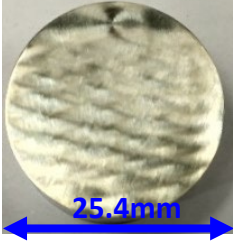

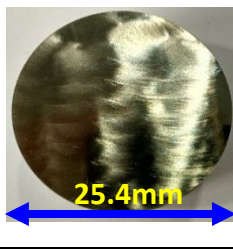
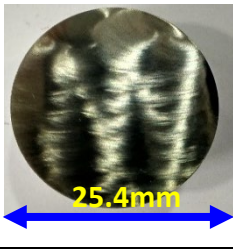
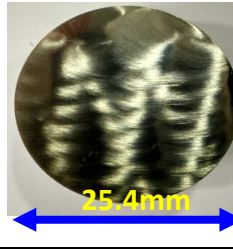
set no.	Photos of samples		
	a	b	c
1			
2			
3			
4			

Table 11 the error maps for pattern tests

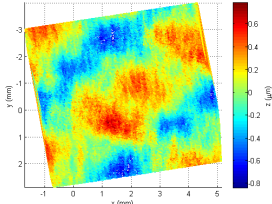
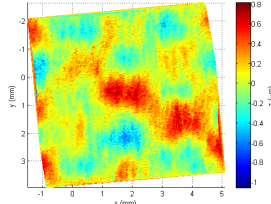
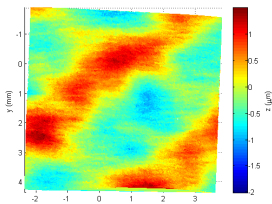
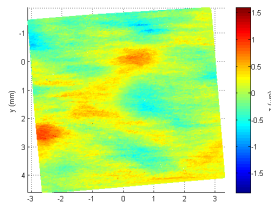
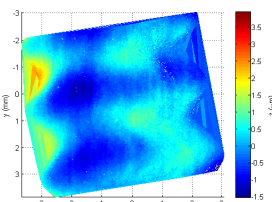
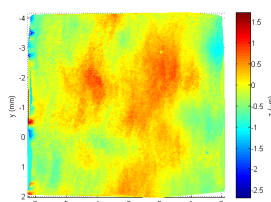
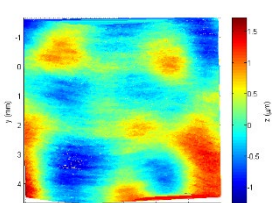
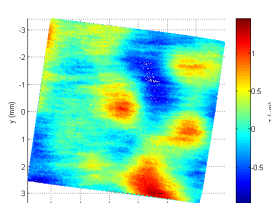
Parameter set no.	The error maps	
	Between measurement data set a and measurement data set b	Between measurement data set a and measurement data set c
1		
2		
3		
4		

Table 12 The root-mean-squared value (RMS) of the error maps for pattern tests

Parameter set no.	The root-mean-squared value of the error maps (μm)	
	Between measurement data set a and measurement data set b	Between measurement data set a and measurement data set c
1	0.2556	0.2221
2	0.5020	0.2528
3	0.5530	0.3330
4	0.4791	0.3710

#### 4.3 Group C: Experimental verification of surface generation model for SPBP

In Group C, a polishing experiment was undertaken to evaluate the performance of the multi-scale material removal model and surface generation model for SPBP. The simulation and polishing experiments were conducted using a swing speed of 250 degrees per minute, a spacing 0.4 mm for the polishing tool path, and the same polishing parameters with pattern tests of set 1 as shown in Table 8. To compare the simulation results and measured results quantitatively, the

measured results have to be registered to the simulated results by a freeform surface characterization method which has been purposely built based on an iterative closest point (ICP) method [22].

To improve the accuracy and robustness of the registration process, the simulated surface was first filtered with a Gaussian zero-order regression filter [23]. Hence, the measured surface was registered to the filtered simulated surface with the ICP method and the transformation matrix was obtained. Based on the calculated transformation matrix, the error map showing the deviation of the simulation results and the measured results was determined by registering the measured results with the original simulated results.

Figure 13 shows the results of the experimental verification of the performance of the multi-scale material removal model and surface generation model for SPBP. As shown in Figure 13(a) and Fig. 13(b), the simulated topography and measured topography of the complex 3D-structured surface generated by SPBP are found to agree well. To further verify the performance of the models quantitatively, the deviation of the measured surface from the corresponding simulated surface was determined by the freeform surface characterization method. Figure 13(c) shows the results after registration of the measured surface and the simulated surface while Figure 13(d) shows the deviation between the simulated and measured results. The simulated results were found to agree reasonably well with the experimental results with the root-mean-squared value (RMS) of the prediction error to be  $0.134\ \mu\text{m}$ . The accuracy of the surface generation model would be further enhanced by increasing the resolution and hence the sample size.

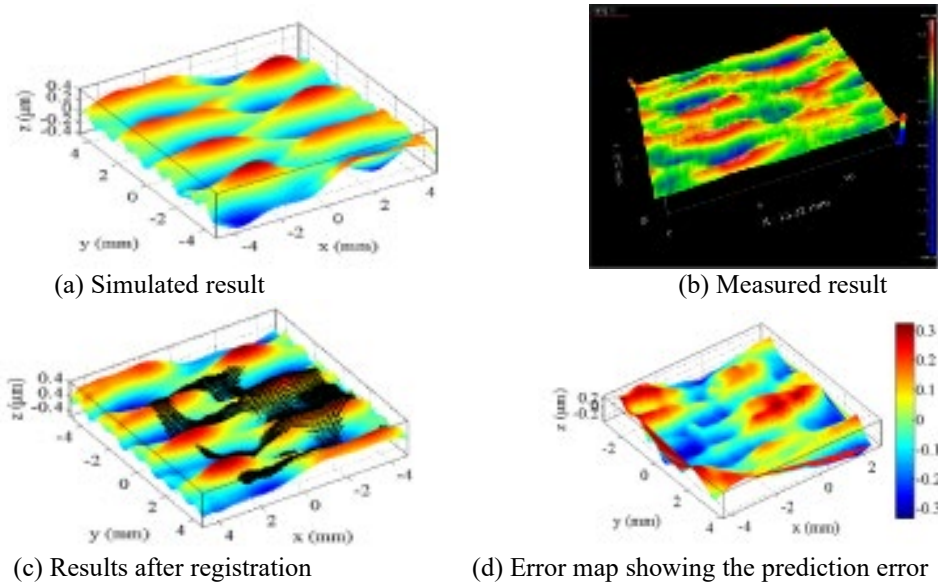


Figure 13. Comparison between the simulated and measured results of swing precess bonnet polishing

## 5. Conclusions

This paper presents a novel swing precess bonnet polishing (SPBP) method for the generation of complex 3D-structured surfaces. SPBP is a sub-aperture finishing process in which the polishing spindle is swung around the normal direction of the target surface within the scope of the swing angle while moving around the center of the bonnet. Line tests of SPBP show that precess angles and the feed rate affect the density of the structures. The smaller the precess angle and the slower the feed rate, the higher the density of the structures. As the precess angle and the feed rate increase, the

Peak-to-valley height (PV) value and the width of a cycle of the 3D-structure increase. The tool offset and swing direction can affect the length of a cycle of the 3D-structure and hence the shape of the 3D-structure. Results of pattern tests were further evaluated and the results show that the range of the RMS values is from  $0.2\mu\text{m}$  to  $0.5\mu\text{m}$ . This infers that the proposed SPBP method can be successfully used for generating different 3D-structured surfaces in deterministic and stable way. A multi-scale material removal model and hence a surface generation model have also been built for characterizing the tool influence function and predicting the 3D-structured surface generation in SPBP based on the study of contact mechanics, kinematics theory, abrasive wear mechanism, and the convolution of the tool influence function and dwell time map along the swing precess polishing tool path. The simulated results were found to agree reasonably well with the experimental results with the root-mean-squared value (RMS) of the prediction error to be  $0.134\mu\text{m}$ .

## Acknowledgement

The work described in this paper was mainly supported by the grants from the Research Grants Council (Project no.: PolyU 5132/11E) and the Innovation and Technology Commission (ITC) (Project no. GHP/031/13SZ) of the Government of the Hong Kong Special Administrative Region (HKSAR), China. The work was also supported by PhD studentships (project code: RTC3 and RTHC) from The Hong Kong Polytechnic University.

## References

- [1] Zhou H, Shan HY, Tong X, Zhang ZH, Ren LQ. The adhesion of bionic non-smooth characteristics on sample surfaces against parts. *Mat Sci Eng a-Struct*. 2006;417:190-6.
- [2] Bechert DW, Bruse M, Hage W, Meyer R. Fluid mechanics of biological surfaces and their technological application. *Naturwissenschaften*. 2000;87:157-71.
- [3] Wakuda M, Yamauchi Y, Kanzaki S, Yasuda Y. Effect of surface texturing on friction reduction between ceramic and steel materials under lubricated sliding contact. *Wear*. 2003;254:356-63.
- [4] Johansen LS, Ginnerup M, Ravnkilde JT, Tang PT, Lochel B. Electroforming of 3D microstructures on highly structured surfaces. *Sensor Actuat a-Phys*. 2000;83:156-60.
- [5] Chen PY, Jywe WY, Wang MS, Wu CH. Application of blue laser direct-writing equipment for manufacturing of periodic and aperiodic nanostructure patterns. *Precis Eng*. 2016;46:263-9.
- [6] Shen JC, Jywe WY, Wu CH. Control of an equipment for fabricating periodic nanostructure. *Precis Eng*. 2014;38:391-7.
- [7] Schaller T, Bohn L, Mayer J, Schubert K. Microstructure grooves with a width of less than  $50\mu\text{m}$  cut with ground hard metal micro end mills. *Precis Eng*. 1999;23:229-35.
- [8] Egashira K, Kumagai R, Okina R, Yamaguchi K, Ota M. Drilling of microholes down to  $10\mu\text{m}$  in diameter using ultrasonic grinding. *Precis Eng*. 2014;38:605-10.
- [9] Schinhaerl M, Smith G, Stamp R, Rascher R, Smith L, Pitschke E, et al. Mathematical modelling of influence functions in computer-controlled polishing: Part I. *Applied Mathematical Modelling*. 2008;32:2888-906.
- [10] Cao ZC, Cheung CF, Ren MJ. Modelling and characterization of surface generation in Fluid Jet Polishing. *Precis Eng*. 2016;43:406-17.
- [11] Evans CJ, Paul E, Dornfeld D, Lucca DA, Byrne G, Tricard M, et al. Material Removal Mechanisms in Lapping and Polishing. *Cirp Ann-Manuf Techn*. 2003;52:611-33.

- [12] Zeng SY, Blunt L. Experimental investigation and analytical modelling of the effects of process parameters on material removal rate for bonnet polishing of cobalt chrome alloy. *Precis Eng.* 2014;38:348-55.
- [13] Namba Y, Shimomura T, Fushiki A, Beaucamp A, Inasaki I, Kunieda H, et al. Ultra-precision polishing of electroless nickel molding dies for shorter wavelength applications. *Cirp Ann-Manuf Techn.* 2008;57:337-40.
- [14] Shiou FJ, Ciou HS. Ultra-precision surface finish of the hardened stainless mold steel using vibration-assisted ball polishing process. *Int J Mach Tool Manu.* 2008;48:721-32.
- [15] Kumar S, Jain VK, Sidpara A. Nanofinishing of freeform surfaces (knee joint implant) by rotational-magnetorheological abrasive flow finishing (R-MRAFF) process. *Precis Eng.* 2015;42:165-78.
- [16] Cheung CF, Kong LB, Ho LT, To S. Modelling and simulation of structure surface generation using computer controlled ultra-precision polishing. *Precis Eng.* 2011;35:574-90.
- [17] Stout KJ, Blunt L. A contribution to the debate on surface classifications - random, systematic, unstructured, structured and engineered. *Int J Mach Tool Manu.* 2001;41:2039-44.
- [18] Beaucamp A, Namba Y. Super-smooth finishing of diamond turned hard X-ray molding dies by combined fluid jet and bonnet polishing. *Cirp Ann-Manuf Techn.* 2013;62:315-8.
- [19] Tam HY, Cheng HB. An investigation of the effects of the tool path on the removal of material in polishing. *J Mater Process Tech.* 2010;210:807-18.
- [20] Cao ZC, Cheung CF. Multi-scale modeling and simulation of material removal characteristics in computer-controlled bonnet polishing. *Int J Mech Sci.* 2016;106:147-56.
- [21] Williams CK, Rasmussen CE. Gaussian processes for machine learning. the MIT Press. 2006;2:4.
- [22] Besl PJ, Mckay ND. A Method for Registration of 3-D Shapes. *Ieee T Pattern Anal.* 1992;14:239-56.
- [23] Brinkmann S, Bodschwinna H, Lemke HW. Accessing roughness in three-dimensions using Gaussian regression filtering. *Int J Mach Tool Manu.* 2001;41:2153-61.